Experimental and Theoretical Studies of Gas-Phase Ion/Molecule Reactions in SiF_4 Forming $SiF_m^+(SiF_4)_n$ Clusters ($m = 0-3$ and $n = 0-2$)

Kenzo Hiraoka,* Masayuki Nasu, Akihito Minamitsu, Akitaka Shimizu, and Daisuke Oomori

Faculty of Engineering, Yamanashi University, Takeda-4, Kofu 400-8511, Japan

Shinichi Yamabe*

Department of Chemistry, Nara University of Education, Takabatake-cho, Nara 630-8528, Japan

Received: July 31, 1998; In Final Form: November 12, 1998

Gas-phase ion/molecule reactions in SiF_4 were studied using a pulsed-electron beam mass spectrometer. The thermochemical stabilities of $SiF_m^+(SiF_4)_n$ have been determined. Owing to the serious charging of the ion source, only up to $n = 2$ thermochemical data could be obtained experimentally. To evaluate bond energies that were difficult to obtain experimentally, ab initio calculations were carried out. Si^+SiF_4 and SiF^+SiF_4 have similar bond energies, 13 kcal/mol. $SiF_2^+SiF_4$ and $SiF_3^+SiF_4$ have 25 and 38 kcal/mol, respectively. While the bond energies of $SiF_m^+(SiF_4)_1$ varied substantially with m, those of $SiF_m^+(SiF_4)_2$ are all ca. 10 kcal/mol. The Si^+SiF_4 geometry is calculated to be a bidentate (bridged) one, where the Si^+ atom is located midway between two Si−F bonds. On the other hand, $SiF_3^+SiF_4$ has a symmetric D_{3d} structure where an F atom is shared equally by two SiF_3 fragments. Theoretical bond energies are in excellent agreement with experimental ones.

1. Introduction

Silane and its halogenated compounds are the most important reagent gases in the field of plasma technology. In particular, silicon fluoride has been extensively studied because it is used to etch and deposit silicon layers in the fabrication of microelectronics devices and solar cells. During etching, highly reactive fluorine radicals and ions present in the plasma impact the surface and volatilize the silicon surface via SiF_4 and SiF_2.

Armentrout et al. studied the energetics and dynamics in the reaction of Si^+ with SiF_4 using guided ion beam mass spectrometry.[1] Absolute reaction cross sections were measured as a function of kinetic energy from thermal to 40 eV. They also measured cross sections as a function of kinetic energy for interaction of N^+, N_2^+, Ar^+, Kr^+, Ne^+, and He^+ with SiF_4.[2,3] Jacox et al. measured the infrared spectra of SiF_3^+ and SiF_3^-, using the matrix isolation method.[4] The results of ab initio calculations of the structures and ground-state vibrational fundamentals of these two ion species were also presented.[4] Schaeffer et al. performed ab initio calculations to determine the molecular structures and total energies of SiF_n and SiF_n^- ($n = 1-5$).[5] The significant measures of neutral-anion separation were pointed out. Ricca and Bauschlicher computed heats of formation for SiF_n and SiF_n^-, for $n = 1-4$. The vibrational frequencies and energetics of these species were determined.[6]

In the present work, ion/molecule reactions between SiF_m^+ and SiF_4 have been investigated both experimentally and theoretically.

2. Experimental and Computational Methods

2.1. Experimental Methods. The experiments were performed with a pulsed electron beam high-pressure mass spectrometer, which has been described previously.[7,8] The reagent gas of He containing 5% of SiF_4 (Sumitomo Seika KK) at about 3 Torr was passed through the molecular sieve 5A trap at dry ice/acetone temperature and then was fed into the ion source. The ions escaping from the field-free ion source into an evacuated region were mass analyzed by a quadrupole mass spectrometer (ULVAC, MSQ-400, $m/z = 1-550$).

In the present experiment, a serious decrease in the ion signals was observed with decrease of ion source temperature. A modest increase in ion intensities was observed when a positive or negative potential was applied to the ion repeller electrode. However, the applied electric field in the ion source made the ion drift velocity so fast that the reliable equilibrium constants could not be determined under such experimental conditions. The decrease in the ion intensities is due to the charging of the surface of the ion source during the experiments. We had similar experience in the O_2 and rare gas experiments.[9,10] It was found that the observed charging effect was moderately suppressed when the surface of the ion source was coated with colloidal graphite. All experimental data presented here were obtained using the graphite-coated ion exit slit. Due to the weak signal intensities, great care was taken to perform reliable measurements.

2.2. Computational Methods. Ab initio calculations of cluster geometries and bond energies for $n = 1$ and 2 were performed using the GAUSSIAN 94 program.[11] Geometries of SiF_m^+ ions, SiF_4, and $SiF_m^+(SiF_4)_n$ clusters were optimized fully with the density-functional theory (DFT) of nonlocal gradient corrections.[12] The Becke 3LYP(B3-LYP)[13,14] functional with the 6-31G* basis set was used for geometry optimization. This method is known to give reliable geometries.[15] B3-LYP/6-31G* vibrational analyses were also carried out to check whether the obtained geometry is located at the stable point and to obtain the zero-point energies (ZPE's). Electronic energies were refined by single-point calculations of the method, B3-LYP/6-311+G(2d,p), B3-LYP/6-311+G(2d,p)//B3-LYP/6-31G*. This is prob-

10.1021/jp983253b CCC: $18.00
Published on Web 01/13/1999

TABLE 1: Thermochemical Data, $-\Delta H^\circ_{n-1,n}$ (kcal/mol) and $-\Delta S^\circ_{n-1,n}$ [cal/(mol K)] for Clustering Reaction 1 with $m = 0-3$[a,b]

	$n=1$		$n=2$		$n=3$	
clustering reaction	$-\Delta H^\circ_{n-1,n}$	$-\Delta S^\circ_{n-1,n}$	$-\Delta H^\circ_{n-1,n}$	$-\Delta S^\circ_{n-1,n}$	$-\Delta H^\circ_{n-1,n}$	$-\Delta S^\circ_{n-1,n}$
$Si^+(SiF_4)_{n-1} + SiF_4 = Si^+(SiF_4)_n$			9.5	19	~5	(20)[c]
	[13.27]		[9.59]			
$SiF^+(SiF_4)_{n-1} + SiF_4 = SiF^+(SiF_4)_n$	12.4	14	9.0	24	~6	(20)[c]
	[12.83]		[9.03]			
$SiF_2^+(SiF_4)_{n-1} + SiF_4 = SiF_2^+(SiF_4)_n$	25.7	18				
	[24.87]		[10.88]			
$SiF_3^+(SiF_4)_{n-1} + SiF_4 = SiF_3^+(SiF_4)_n$	≥35		10	21	~5	(20)[c]
	[37.66]		[10.58]			
$SiF_3OH_2^+(SiF_4)_{n-1} + SiF_4 = SiF_3OH_2^+(SiF_4)_n$	9.6	15	7.7	19	~5	(20)[c]

[a] Experimental errors for ΔH° and ΔS° values are 0.3 kcal/mol and 3 cal/(mol K), respectively. [b] Enthalpy changes in square brackets are theoretical energies evaluated with B3-LYP/6-311+G(2d,p)//B3-LYP/6-31G* electronic energies, B3-LYP/6-31G* zero-point vibrational ones, and temperature corrections. [c] Entropy value assumed, and thus, $\Delta H^\circ_{n-1,n}$ must be regarded as only an approximate value.

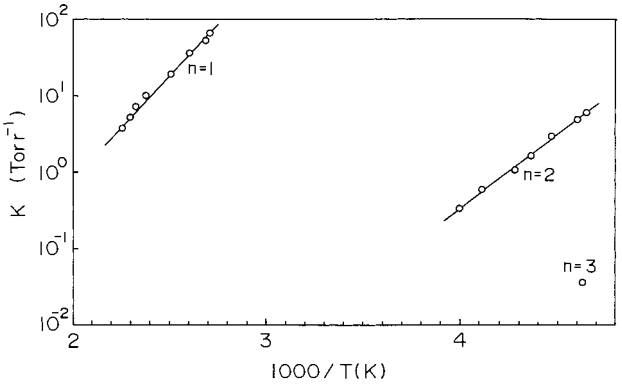

Figure 1. The van't Hoff plots for the clustering reaction, $SiF^+(SiF_4)_{n-1} + SiF_4 = SiF^+(SiF_4)_n$.

ably the most practical way to determine cluster geometries of the present systems. Theoretical bond energies (enthalpy changes) were estimated by the difference of B3-LYP/6-311+G(2d,p) electronic energies, B3-LYP/6-31G* ZPEs, and temperature corrections. All the calculations were performed on the CONVEX SPP-1200/XA computer at the Information Processing Center of the Nara University of Education.

3. Experimental Results

When the reagent gas of He containing 5% of SiF_4 at about 3 Torr was ionized by 2 keV electrons, SiF_m^+ with $m = 0-3$ were observed as primary ions. The equilibria of reaction 1 for Si^+ ($m = 0$) and $n = 1$ could not be measured because of the weak signal intensity of Si^+ and its rapid decay after the ionizing electron pulse.

$$SiF_m^+(SiF_4)_{n-1} + SiF_4 = SiF_m^+(SiF_4)_n \qquad (1)$$

As an example, van't Hoff plots for reaction 1 with $m = 1$ are shown in Figure 1. In Table 1, the enthalpy and entropy changes obtained from the van't Hoff plots are summarized.

Si^+ was known to be unreactive toward SiF_4 at thermal energy.[16] This is in accord with the calculated small bond energy of 13.3 kcal/mol for Si^+SiF_4 (see Table 1); i.e., the interaction is noncovalent but electrostatic. For SiF^+, the equilibria for reaction 1 could be observed successfully. For SiF_2^+, the equilibria with $n \geq 2$ could not be measured because of the presence of impurity in the system.

In the measurement of the equilibria for reaction 1 for SiF_3^+ ($m = 3$), the intensity of $SiF_3^+(SiF_4)_1$ was found to be larger than that of SiF_3^+ at the highest temperature measured (690 K) and the equilibrium for reaction 1 with $n = 1$ could not be measured. The bond energy of $SiF_3^+SiF_4$ may be estimated to be ≥35 kcal/mol. It is worthwhile to note that the bond energy of $SiF_3^+SiF_4$ is much larger that of isovalent $CF_3^+CF_4$, 6.6 kcal/mol.[17] The characteristic difference in the nature of bonding between these isovalent complexes will be discussed in the following theoretical section.

In the present experiments, the formation of SiF_4^+ and its cluster ions could not be observed. Armentrout and co-workers reported that SiF_4^+ is the major product ion in reactions of thermal N_2^+ and Ar^+ ions with SiF_4.[2,3]

$$N_2^+ + SiF_4 = SiF_4^+ + N_2 \qquad (2)$$

$$Ar^+ + SiF_4 = SiF_4^+ + Ar \qquad (3)$$

To produce SiF_4^+, 50−80% of N_2 or Ar gas was added to the reagent gas of He/SiF_4(95/5) at the total pressure of about 3−4 Torr. Since the major ions He^+ may produce the N_2^+ or Ar^+ ion by the charge-transfer reaction, reaction 2 or 3 must take place in the mixture of N_2 or Ar with He/SiF_4. Ignacio and Schlegel reported a Hartree−Fock geometry for SiF_4^+ starting from the T_d structure for SiF_4.[18] Upon $SiF_4SiF_4^+$, one Si−F bond is greatly elongated with a small distortion of the remaining SiF_3 subunit. Ricca and Bauschlicher performed the 2-pt(TZ,−QZ) calculations on SiF_4^+. They found that SiF_3^+F is weakly bound and easily dissociates into SiF_3^+ and F.[6] The calculated bond energy of SiF_3^+F was 19 kcal/mol.[6] Because this value is much smaller than the estimated bond energy of $SiF_3^+SiF_4$ (≥35 kcal/mol), SiF_4^+ may experience the displacement reaction 4 with SiF_4 under the present experimental conditions.

$$SiF_4^+ + SiF_4 \rightarrow SiF_3^+(SiF_4)_1 + F \qquad (4)$$

Actually, Reents and Mujsce found that reaction 4 does take place with the rate constant of 3.6×10^{-10} cm^3/(molecule•s) at 373 K.[16]

In the present experimental system, the formation of ion with $m/z = 103$ (one mass unit smaller than SiF_4^+) was observed. The rate of the formation of this ion was apparently slower than those of the primary ions SiF_m^+. This ion was assigned to be $SiF_3^+OH_2$ because its intensity was found to increase with an addition of a small amount of water in the gas handling system. This ion may be formed either by the recombination reaction of SiF_3^+ with water impurity or by the displacement reaction of the cluster ions of SiF_3^+ with H_2O. The thermochemical values for clustering reaction 5 are given in Table 1.

$$SiF_3OH_2^+(SiF_4)_{n-1} + SiF_4 = SiF_3OH_2^+(SiF_4)_n \qquad (5)$$

4. Theoretical Results and Discussion

To determine cluster geometries of $SiF_m^+(SiF_4)_n$ and to assess the experimental binding energies, $-\Delta H^\circ_{n-1,n}$, ab initio calcu-

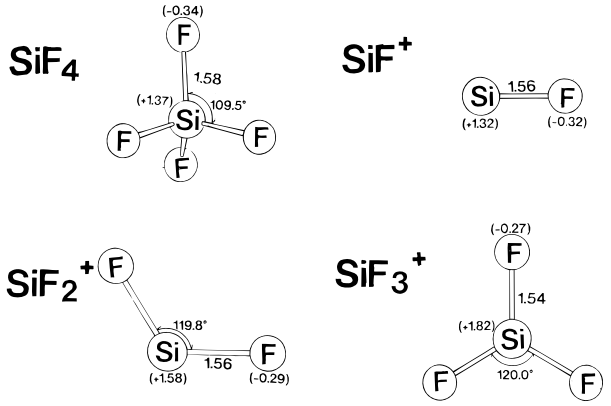

Figure 2. Geometries of cluster component molecules optimized by the B3-LYP/6-31G* method. Distances are in angstrom, and numbers in parentheses denote Mulliken electronic net charges (positive, cationic).

lations have been made. Figure 2 exhibits geometries of their component species. Since electronegativities of Si (1.8) and F (4.0) atoms are significantly different, Si−F bonds are quite polar. Even in SiF_4, the silicon atom is very cationic (+1.37). It is interesting that the polarity of $Si-F^+$ is similar to that of SiF_4. The monocation character of SiF^+ may be roughly attributable to the silicon atom (with three valence electrons). Two electron configurations of SiF^+ are conceivable.

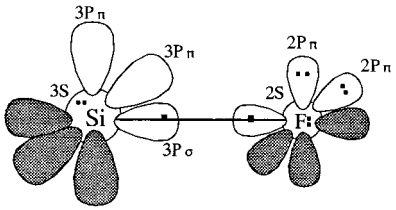

singlet
(closed subshell)

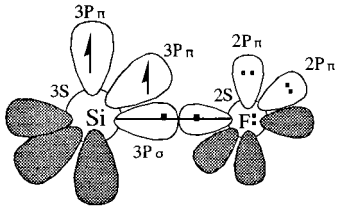

triplet
(open subshell)

In the singlet spin state, three valence electrons of Si^+ are assigned to the configuration $3s^23p_\sigma^1$. In the triplet spin state, they are to assigned $3p_\pi^13p_\pi^13p_\sigma^1$. In the former configuration, the energetic stability of 3s > 3p is used, but Hund's rule is ineffective. In the latter configuration, vice versa. The SiF^+ species of both spin states have been calculated, and their energies are compared. The singlet spin state is found to be much more stable than the triplet spin state by 109.1 kcal/mol, B3-LYP/6-31G*. Consequently, the electrophilic character is oriented perpendicularly to the Si−F axis.

SiF_2^+ has 17 valence electrons and has a bent structure according to the Walsh rule.[19] The geometry of SiF_2^+ is also shown in Figure 2. The bond angle, 119.8°, indicates that the silicon atom is sp^2 hybridized and has the following electron configuration. SiF_2^+ is a σ radical with a vacant $3p_\pi$ orbital.

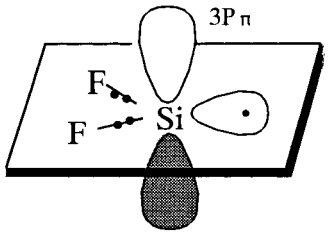

SiF_2^+ is electrophilic to the out-of-plane direction.

SiF_3^+ has 24 valence electrons and, accordingly, a planar geometry by the Walsh rule. The geometry is shown in Figure 2, which is regarded as that constructed by $SiF_2^{\bullet+} + {}^\bullet F$. Therefore, the electrophilic character is oriented to the out-of-plane direction. The silicon atom is very cationic (+1.82).

On the basis of those geometries and electron configurations of fragment species in Figure 2, the $SiF_m^+(SiF_4)_1$ geometries may be predicted.

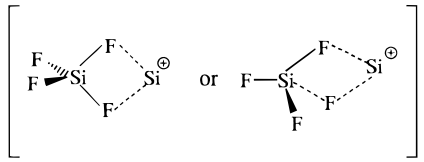

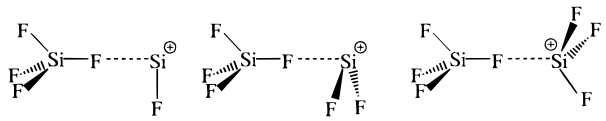

Figure 3 shows geometries of $Si^+(SiF_4)_n$ with $n = 1$ and 2. $Si^+(SiF_4)_1$ has a C_{2v} symmetry, where the silicon atom is bidentately coordinated to SiF_4. The bridge F···Si distance is large, 2.28 Å; however, the electronic charge is shifted to some extent, $SiF_4 \rightarrow Si^+$.

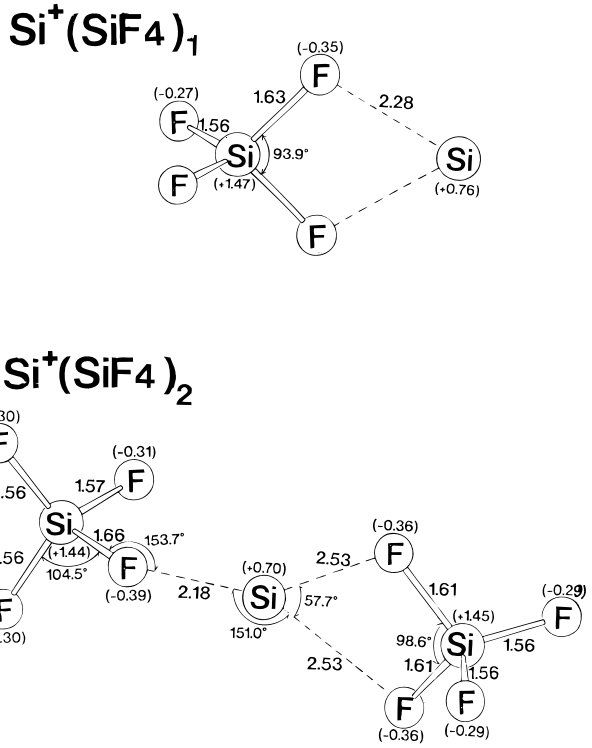

Figure 3. Geometries of $Si^+(SiF_4)_n$, $n = 1$ and 2.

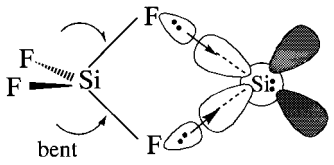

To cause the bridge and dual charge-transfer interactions, the odd electron is situated at the out-of-plane $3p_\pi$ orbital. The second SiF_4 is attracted by $(SiF_4)Si^+$ monodentately. Different from $Si^+(SiF_4)_1$, the one-site interaction of $Si^+(SiF_4)_2$ arises from the exchange repulsion. A double chelate coordination is found to be absent.

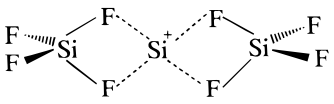

Since the Si^+ atom is not assisted by the fluorine substituents, its electrophilicity is not large. In fact, interaction distances shown by broken lines in Figure 3 are large.

Figure 4 shows geometries of $SiF^+(SiF_4)_n$ ($n = 1$ and 2). As expected by the electron configuration of SiF^+, a perpendicular coordination $F-Si^+ \leftarrow F-SiF_3$ has been obtained. One F−Si bond of SiF_4 is elongated considerably by the coordination. The $SiF^+(SiF_4)_2$ geometry is also in line with that predicted in terms of the SiF^+ electron configuration. The intermolecular bond angle, 80.9°, is noteworthy, which is expected to be 90° for two orthogonal $3p_\pi$ orbitals. The following secondary attraction decreases the angle. Here, the secondary attraction means a ligand−ligand or ligand−terminal atom interaction.

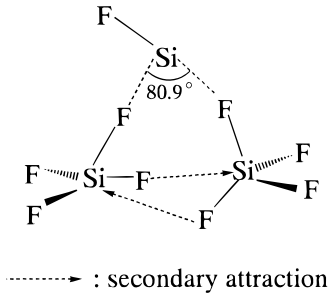

Figure 5 exhibits geometries of $SiF_2^+(SiF_4)_n$ ($n = 1$ and 2). As expected, the $3p_\pi$ atomic orbital of SiF_2^+ is coordinated by one Si−F bond of SiF_4. Two SiF bonds have similar distances, 1.74 and 1.84 Å in $n = 1$, which indicates that the $SiF_4 \rightarrow SiF_2^+$ charge-transfer interaction is strong. The second SiF_4 molecule is linked with the backside of the $SiF_2^+(SiF_4)_1$ cluster. Two SiF_4 ligands are found to be equivalent with respect to the SiF_2^+ center. The apparent steric crowded geometry (cis configuration of two SiF_4 ligands) comes from the secondary SiF attraction.

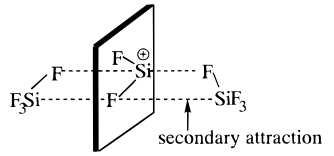

Figure 6 presents geometries of $SiF_3^+(SiF_4)_n$ ($n = 1$ and 2). Owing to the strongest electrophilic character of SiF_3^+ among SiF_m^+ cation species, the $SiF_3^+(SiF_4)_1$ cluster is found to have a symmetric (D_{3d}) geometry. Experimentally, a large (≥35 kcal/mol) bond energy has been predicted, and the difficulty of

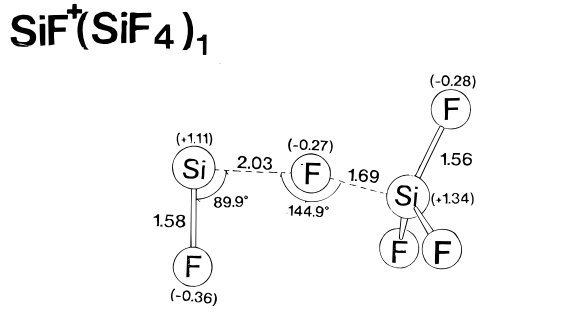

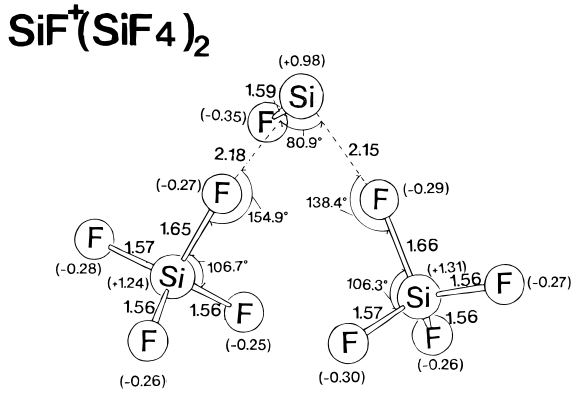

Figure 4. Geometries of $SiF^+(SiF_4)_n$, $n = 1$ and 2.

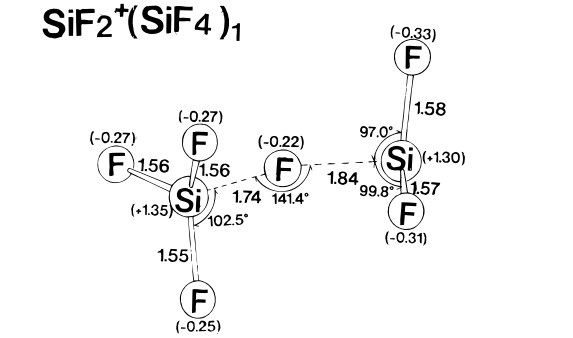

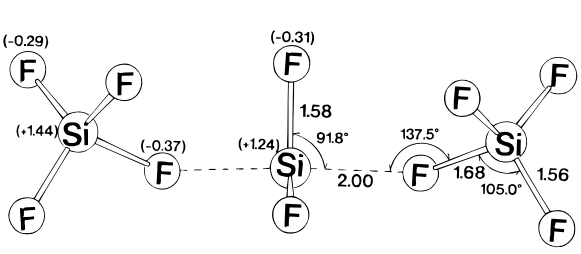

Figure 5. Geometries of $SiF_2^+(SiF_4)_n$, $n = 1$ and 2.

gaining the accurate van't Hoff plot of $n = 0 \rightarrow 1$ is understandable by the D_{3d} symmetric structure. The $SiF_3^+(SiF_4)_2$ species is also of a symmetric (D_{3d}) geometry, which is similar to the equivalent coordination of two SiF_4 molecules to the SiF_3^+ center. For $SiF^+(SiF_4)_2$ and $SiF_2^+(SiF_4)_2$ clusters, such equivalent and weaker (than the $n = 0 \rightarrow 1$ reaction) coordination has been obtained. Energy falloffs of $-\Delta H^\circ_{0,1} \rightarrow -\Delta H^\circ_{1,2}$ are expected, in particular for $SiF_3^+(SiF_4)_n$.

The difference of bond energies between $CF_3^+(CF_4)_1$ and $SiF_3^+(SiF_4)_1$ is reflected in asymmetric and symmetric structures, respectively.

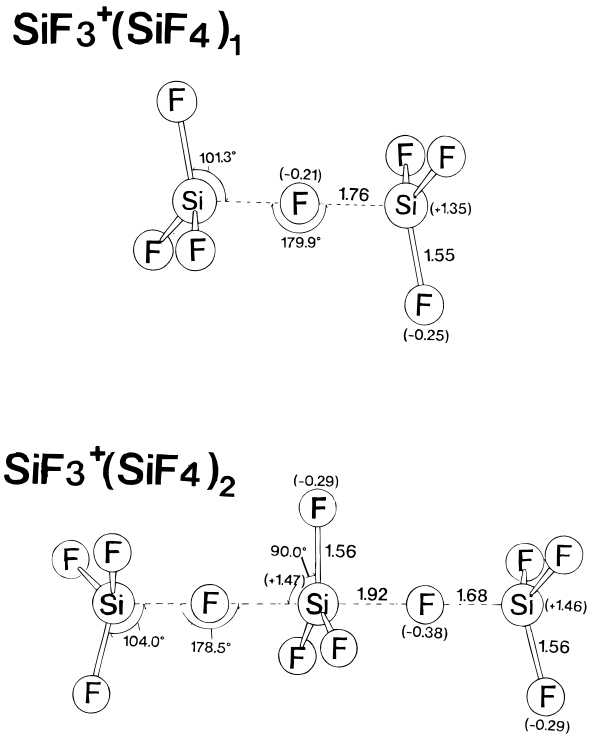

Figure 6. Geometries of $SiF_3^+(SiF_4)_n$, $n = 1$ and 2.

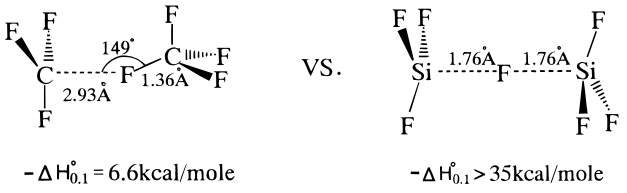

While $-\Delta H^\circ_{0,1} = 6.6$ kcal/mol of $CF_3^+(CF_4)_1$ corresponds to a weak $CF_3^+\cdots CF_4$ intermolecular interaction, $-\Delta H^\circ_{0,1} > 35$ kcal/mol for $SiF_3^+(SiF_4)_1$ does to the formation of a semicovalent bond. This drastic difference is attributable mainly to the electrophilicities of CF_3^+ and SiF_3^+. There is a hyperconjugation between p_π orbitals.

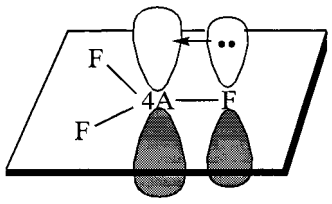

4A = C or Si

When the conjugation is strong, the elecrophilicity of the central atom is lowered and the C−F (or Si−F) bond is shortened. The C−F distances of CF_4 and CF_3^+ are 1.30 and 1.22 Å, respectively. The Si−F ones of SiF_4 and SiF_3^+ are 1.58 and 1.54 Å, respectively (Figure 2). Obviously, CF_3^+ has a larger hyperconjugation and a poorer electrophilicity than SiF_3^+. The extent of mixing of $2p_\pi$(C) and $2p_\pi$(F) orbitals is larger than that of $3p_\pi$(Si) and $2p_\pi$(F) ones, leading to the larger conjugation in CF_3^+.

Table 1 displays theoretical bond energies in square brackets. They are in good agreement with the present experimental energies. While $-\Delta H^\circ_{0,1}$ values differ significantly according to the electrophilicity of SiF_m^+, $-\Delta H^\circ_{1,2}$ ones are about 10 kcal/mol.

Determination of thermochemical data of $SiF_m^+(SiF_4)_n$ has been an extremely difficult task due to the serious charging of the ion source. This work has demonstrated that the combination of careful measurements and accurate calculations is indispensable for such difficult targets of gas-phase ion−molecule reactions.

References and Notes

(1) Weber, M. E.; Armentrout, P. B. *J. Chem. Phys*. **1988**, *88*, 6898.

(2) Kickel, B. L.; Fisher, E. R.; Armentrout, P. B. *J. Phys. Chem*. **1993**, *97*, 10198.

(3) Weber, M. E.; Armentrout, P. B. *J. Chem. Phys*. **1989**, *90*, 2213.

(4) Jacox, M. E.; Irikura, K. K.; Thompson, W. E. *J. Chem. Phys*. **1995**, *103*, 5308.

(5) King, R. A.; Mastryukov, V. S.; Schaeffer, H. F. *J. Chem. Phys*. **1996**, *105*, 6880.

(6) Ricca, A.; Bauschlicher, C. W., Jr. *J. Phys. Chem*. **1998**, *102*, 876.

(7) Kebarle, P. In *Techniques for the Study of Ion−Molecule Reactions*; Farrar, J. M., Saunders, W. H., Eds.; Wiley: New York, 1988.

(8) Hiraoka, K. *J. Chem. Phys.* **1987**, *87*, 4048.

(9) Hiraoka, K. *J. Chem. Phys.* **1988**, *89*, 3190.

(10) Hiraoka, K.; Mori, T. *J. Chem. Phys.* **1989**, *90*, 7143.

(11) Frisch, M. J.; Trucks, G. W.; Schlegel, H. B.; Gill, P. M. W.; Johnson, B. G.; Robb, M. A.; Cheeseman, J. R.; Keith, T.; Petersson, G.; Foresman, J. B.; Cioslowski, J.; Stefanov, B. B.; Nanayakkara, A.; Challacombe, M.; Peng, C. Y.; Ayala, P. Y.; Chen, W.; Wong, M. W.; Andres, J. L.; Replogle, E. S.; Gomperts, R.; Martin, R.L.; Fox, D. J.; Binkley, J. S.; Defrees, D. J.; Baker, J.; Stewart, J. P.; Head-Gordon, M.; Gonzalez, C.; Pople, J. A. *Gaussian 94, Revision C.4*; Gaussian, Inc.: Pittsburgh, PA, 1995.

(12) Parr, R. G.; Yang, W. *Density-Functional Theory of Atoms and Molecules*; Oxford University Press: New York, 1989.

(13) Becke, A. D. *J. Chem. Phys.* **1993**, *98*, 5648.

(14) Lee, C.; Yang, W.; Parr, R. G. *Phys. Rev. B* **1988**, *37*, 785.

(15) Foresman, J. B.; Frisch, Æleen, *Exploring Chemistry with Electronic Structure Methods*, 2nd ed.; Gaussian Inc.: Pittsburgh, PA, 1996; p 146.

(16) Reents, W. D., Jr.; Mujsce, A. M. *Int. J. Mass Spectrom. Ion Processes* **1984**, *59*, 65.

(17) Hiraoka, K.; Nasu, M.; Fujimaki, S.; Ignacio, E. W.; Yamabe, S. *J. Phys. Chem*. **1996**, *100*, 5245.

(18) Ignacio, E. W.; Schlegel, H. B. *J. Phys. Chem.* **1990**, *94*, 7439.

(19) Walsh, A. D. *J. Chem. Soc.* **1953**, 2269.